

Prediction of notch strength ratio of a notched tensile ductile iron using multiple linear regression model

Gülcan TOKTAŞ*

Balıkesir University, Faculty of Engineering, Department of Mechanical Engineering.

Geliş Tarihi (Received Date): 28.01.2025

Kabul Tarihi (Accepted Date): 28.02.2025

Abstract

This study aims to create a model by examining the effect of the matrix structure and notch root radius on the notch strength ratio (NSR) in an alloyed ductile cast iron through multiple linear regression analysis. For this purpose, several heat treatments were applied to obtain ferritic, pearlitic/ferritic, pearlitic, tempered martensitic, lower bainitic, and upper bainitic matrix structures in cast iron. Hardness and tensile tests were applied to determine the hardness and 0.2 yield strength of matrix structures, which were then considered independent variables in the regression analysis. Additionally, tensile tests were conducted on circumferentially V-notched samples with a notch root radius range of 0.05-0.8 mm, and the notch radius was used as the third independent variable in the analysis. A model was developed by multiple regression to predict the NSR with the aid of the hardness, 0.2 yield strength, and notch radius independent variables. The analysis had an adjusted R^2 value of 0.886, which explains that 88.6 % of predicted NSR values can be varied by the hardness, 0.2 yield strength, and notch root radius. The model predicted satisfactory NSR values in matrix structures, exhibiting only minimal residuals.

Keywords: Ductile iron, matrix structure, regression analysis, notch strength ratio.

Sünek dökme demirde çentik mukavemet oranının çoklu doğrusal regresyon modeli ile tahmini

Öz

Bu çalışmada, alaşımlı sünek dökme demirde matris yapısı ve çentik kök yarıçapının çentik mukavemet oranına olan etkisi çoklu doğrusal regresyon analizi ile incelenerek bir

* Gülcan TOKTAŞ, gzeytin@balikesir.edu.tr, <https://orcid.org/0000-0002-0455-2107>

model oluşturulması hedeflenmiştir. Bu amaçla, dökme demirde ferritik, perlitik/ferritik, perlitik, temperlenmiş martensitik, alt bey nitik ve üst bey nitik matris yapıları elde etmek için çeşitli ısıl işlemler uygulanmıştır. Matris yapıların sertliğini ve 0,2 akma dayanımını belirlemek için sertlik ve çekme testleri uygulanmış ve bunlar regresyon analizinde bağımsız değişkenler olarak ele alınmıştır. Ayrıca, 0,05-0,8 mm çentik kök yarıçapı aralığına sahip çevresel V çentikli numuneler üzerinde çekme testleri uygulanmış ve elde edilen çentikli çekme dayanımları regresyon analizinde üçüncü bağımsız değişken olarak kullanılmıştır. Sertlik, 0,2 akma dayanımı ve çentik kök yarıçapı bağımsız değişkenleri ile çentik mukavemet oranını tahmin etmek için çoklu regresyon analizi yardımıyla bir model geliştirilmiştir. Analiz sonucunda, 0,886 değerinde ayarlanmış bir R^2 değeri elde edilmiştir. Bu sonuç, tahmin edilen çentik mukavemet oranı değerlerinin %88,6'sının sertlik, 0,2 akma dayanımı ve çentik kök yarıçapı ile değiştirilebileceğini açıklamaktadır. Elde edilen model ile, matris yapılarında yalnızca minimal farklar sergileyen tatmin edici çentik mukavemet oranları öngörülmüştür.

Anahtar kelimeler: Sünek dökme demir, matris yapı, regresyon analizi, çentik mukavemet oranı.

1. Introduction

Ductile irons are not a single material; they are a family of materials that exhibit a wide range of properties achieved through microstructure control [1]. The common feature in all types is the nodular shape of graphite in their microstructure. These nodules prevent the spreading of cracks, making ductile iron tougher and more ductile than gray cast iron. The mechanical properties of these cast irons are determined by the characteristics of the nodules they contain (nodule count, nodularity, and nodule size) and the matrix structure. Due to their comparable properties to many types of steel, such as high strength and toughness, they are successfully used in a wide range of engineering applications. Due to their high strength and shock absorption capabilities, they are used in the automotive industry as crankshafts, gears, and suspension systems parts. Because of corrosion resistance, durability, and ease of installation, they are preferred in the pipeline industry as water and sewage systems. The toughness and machinability properties allow them to be used in the construction and heavy machinery industry such as pump housing and valve bodies [2].

A broad range of industrial and academic studies have been conducted to date on casting, heat treatment, surface treatments, microstructure, and mechanical properties owing to the exceptional properties of this cast iron family. Casting methods, alloying elements, and heat treatments modify the microstructure, consequently impacting mechanical qualities. The mechanical properties of ductile iron play a vital role in material selection, optimizing designs, ensuring safety, and achieving cost-effectiveness. Therefore, it becomes necessary to conduct tests per related standards for designing a part of ductile iron whose mechanical properties are unknown. Sometimes, mechanical tests may not be performed due to a lack of equipment or its calibration, a shortage of qualified personnel, a lack of time, or any other reason. In this case, machine learning can model the mechanical properties using existing variables. Machine learning algorithms derive insights from data to generate predictions or judgments autonomously. Regression is a statistical technique utilized largely for forecasting and prediction, and is strongly associated with the application of machine learning [3]. Regression is performed to

determine the relationship between dependent and independent variables and develop a prediction line and equation that best suits this relationship [4].

Multiple regression analysis is an effective instrument in materials science for elucidating relationships among numerous factors influencing material behavior [5]. It aids in anticipating material characteristics, refining processing parameters, identifying critical factors, and simulating complex interactions. This ultimately results in improved material development, design, and failure mitigation, rendering it an indispensable instrument in both research and industrial applications.

Using multiple regression analyses, many studies have tried to create models that can predict the mechanical properties of ductile iron. Kasvayee et al. [6] looked at how solidification and silicon content affect the mechanical qualities of high silicon ductile iron. They used multiple regression analysis to predict how the iron would behave under tension based on its microstructure. Dix et al. [7] used linear regression analysis to find a link between the processing factors that affect the iron's static mechanical properties and the microstructure that affects those properties for lightweight thin-walled ductile iron. Based on nearly 2000 collected data, Biswas et al. [8] studied cast irons (gray and ductile iron). They classified these data based on their chemical composition and section thickness so that they could statistically look at the hardness and tensile properties of each iron by their composition and section size and then predict mathematical models. In the end, they found that the predicted models for ductile iron had less percent error than those for gray iron. According to Franzen et al. [9], the graphite phase factors (particle count, nodule count, nodule size, and nodule distance) affect Charpy impact energies and the ductile to brittle transition curves in ductile iron. When they looked at the graphite particle count instead of the graphite nodule count, they found that the Charpy impact energy and hardness had a stronger and statistically significant relationship. The regression analysis also showed that the transition temperature was significantly linked to the microstructural factors. Laine et al. [10] modeled the yield and ultimate strength using the silicon content, pearlite fraction, and testing temperature variables. Ram and Gautam [11] studied the impacts of alloying elements on nodularity, hardness, ductility, and tensile strength by regression analysis. However, these studies mostly searched and carefully showed how the solidification parameters, chemical composition, microstructural parameters, testing temperatures, and mechanical properties are related. In terms of statistics, they didn't look at how the shapes of the notches affect the mechanical properties of ductile iron.

Notches may be present in various geometries, such as V, U, elliptic, cornered, circular, etc. These are all made deliberately during the manufacturing process. Also, there can be constituents such as inclusions, lamellae graphites, voids, cracks, and segregations formed unconsciously in the microstructure during solidification, that act as notches. Regardless of how they are formed, all notches create high local stresses in the notch region under the applied external force. Also, the positions of these notches within the material or on the part geometry are important. Same notches can behave differently in the same materials with the same chemical composition but with different matrix structures. In this case, since the chemical composition is ruled out, the mechanical properties of the matrix structure (hardness, yield strength, and tensile strength) determine the behavior of the notch. The stress concentration factor (K_t) is usually used to characterize the notch behavior. The sharpest notches give high-stress concentrations at the notch tips with high K_t values, having higher local stresses than the nominal stress. These stresses often facilitate crack formation and cause the part to break earlier than

expected. In materials with high ductility, these local stresses can cause the crack tip to strengthen through plastic deformation, resulting in higher strength. In this case, the weakening or strengthening effect of the notch may not be understood by the K_t value. The notch strength ratio (NSR), a ratio of the notched tensile strength to the unnotched tensile strength, is used to determine the evidence of strengthening or weakening under static loading. If NSR is smaller than 1, it indicates weakening, as in ceramics, close to 1, notch insensitive, as in metallic glasses, and greater than 1, the strengthening effect as in ductile crystalline materials [12].

This study aimed to search the effects of mechanical properties of matrix structures (hardness, 0.2 yield strength) and notch radius on the NSR values in ductile iron. The main goal is to model the NSR with dependent variables of hardness, 0.2 yield strength, and notch radius using multiple linear regression analysis. Ductile iron was subjected to various heat treatments to eliminate the chemical composition effect, followed by the hardness and tensile tests performed before analysis to have several hardness and 0.2 yield strength variables.

2. Materials and method

The chemical composition of the alloyed ductile iron is given in Table 1. The circumferentially notched tensile specimens were machined from the 25 mm diameter and 400 mm length rods. The specimens have 60° angled and 1 mm depth of V notches with 0.05, 0.1, 0.16, 0.25, 0.4, and 0.8 mm root radii. The specimen's geometry is given in Fig. 1. After machining, the notch radii were measured with a Mitutoyo profile projector (Japan) device at 50X magnification with a precision of 0.005 mm.

Table 1. Chemical composition of the ductile iron (wt.%).

C	Si	Mn	P	S	Mg	Cu	Ni	Mo	Fe
3.73	2.55	0.3	0.045	0.023	0.44	1.03	1.25	0.18	balance

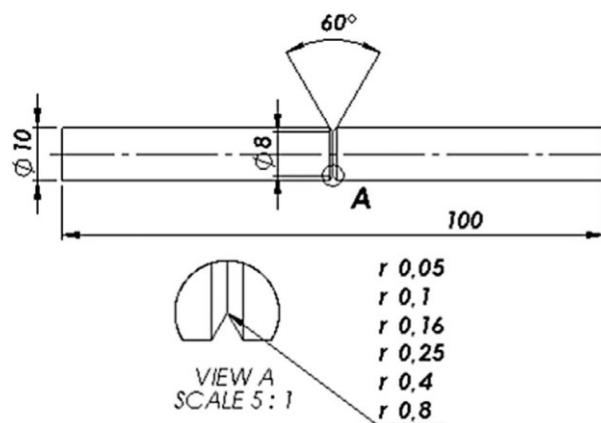


Figure 1. The sketch of the circumferentially notched tensile specimen.

Different heat treatments were applied to get various matrix structures and mechanical properties in the sole chemical composition to eliminate the effect of ductile iron's composition on the regression analysis. The matrix structures are ferritic (F), pearlitic/ferritic (P/F), pearlitic (P), tempered martensitic (TM), lower bainitic (LB), and

upper bainitic (UB). For the F structure, specimens were homogenized at 925 °C for 7 hours, cooled in an electrical furnace until 500 °C, and left in the air. The specimens were held at 900 °C for an hour in a neutral bath, cooled until 660°C at a 2.4 °C/min cooling rate, and cooled in steady air for the P/F matrix. The Pstructure was obtained by holding the specimens at 900 °C for an hour in the neutral bath, cooled until 650 °C at 5 °C/min cooling speed, and cooled in steady air. The specimens were held at 900 °C for an hour, quenched in 80 °C heated oil, and tempered at 400 °C for an hour for the TM structure. The LB and UB structures were obtained by austenitizing at 900 °C for an hour, and held in a salt bath for an hour at 300 °C and 365 °C, respectively.

The surfaces of heat-treated specimens (with 10 mm diameter and 10 mm height) were prepared by the standard metallographic techniques, and etched with 2 % nital solution for the microstructural analysis by an Olympus microscope (Japan). The Brinell hardness tests were performed by applying a 187.5 kg load with a 2.5 mm diameter steel ball for 20 seconds per the ISO 6506-1 standard [13]. The surfaces were ground and polished before the hardness tests. Hardnesses were identified by averaging five values. The tensile tests were performed on the notched and unnotched specimens with 1 mm/min cross-head speed at room temperature. For each condition, five samples were tested and the values were averaged. The applied test procedure of the study is given in Figure 2.

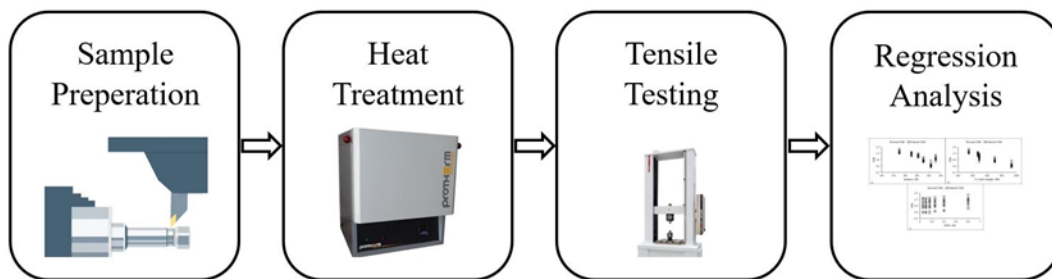


Figure 2. The applied test procedure.

After tests, multiple linear regression analysis was applied to determine the effect of hardness, 0.2 yield strength, and notch root radius (assumed as independent variables) on the NSR (dependent variable). As the matrix structure fully affects the hardness and yield strength, the contribution of microstructure in the analysis was considered in these properties. The analysis was conducted using Excel software at a confidence level of 95 %.

3. Results and discussions

The microstructures of the as-cast ductile iron with and without etching are given in Fig. 3. The cast structure is a bull's eye pearlitic due to the ferrite phase surrounding the nodules dispersed in the pearlitic matrix. The nodularity is above 90 percent, the nodule diameter is 32 μm , and the nodule count is 120 nodule/ mm^2 .

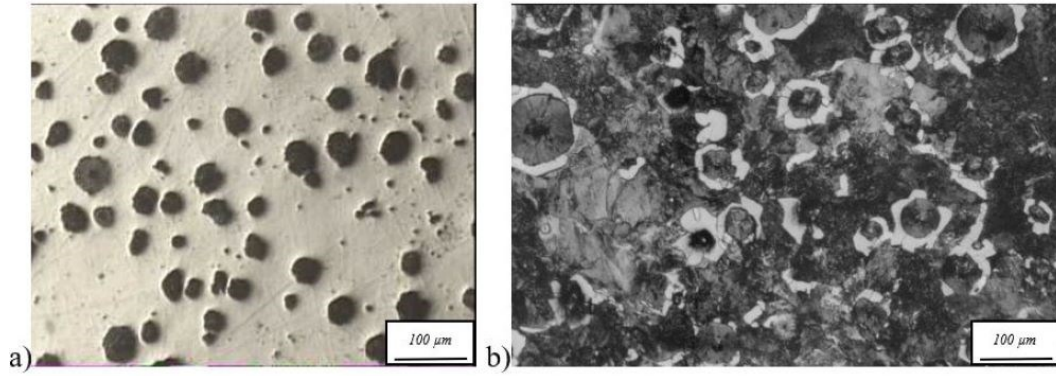


Figure 3. a) unetched and b) etched microstructures of the as-cast ductile iron.

The micrographs of F, P/F, P, TM, LB, and UB matrix structures are given in Fig. 4. The homogenization treatment provided a fully ferritic matrix due to slow cooling in the furnace (Fig. 4a). The cooling rate of 2.4 °C/min from 900 °C to 660 °C formed some pearlite in the ferritic structure (Fig. 4b). Increasing the cooling rate to 5 °C/min increased the pearlite amount. Almost a fully pearlitic structure is seen in Fig. 4c. While fine needle ferrite (dark areas) and high carbon retained austenite (white areas) are formed by austempering at 300 °C, a rougher structure is formed at 365 °C due to high diffusion condition.

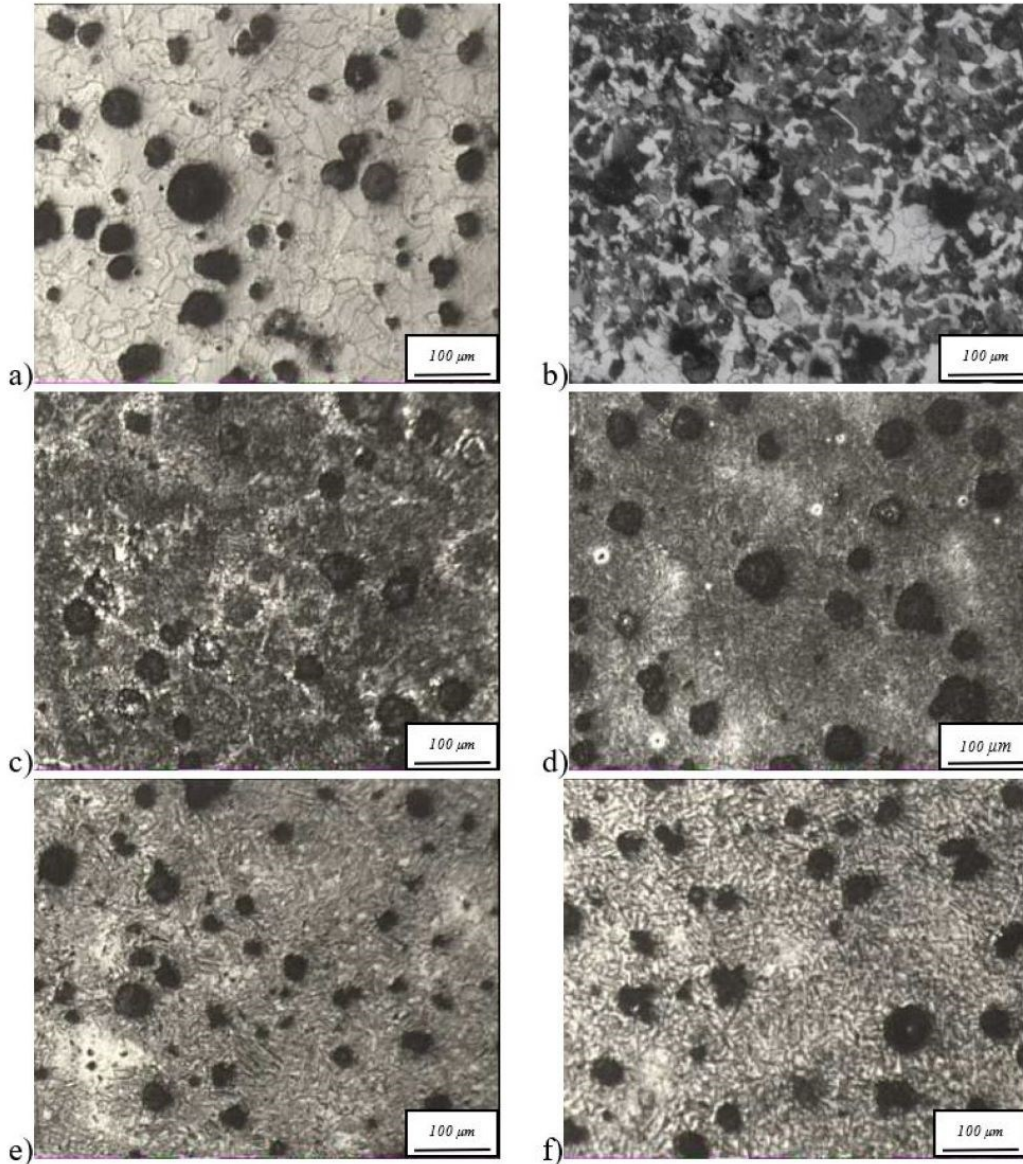


Figure 4. The microstructures of matrix structures
 a) F, b) P/F, c) P, d) TM, e) LB, and f) UB.

The hardness, 0.2 yield, and ultimate tensile strengths of the unnotched specimens are given in Table 2. Since the ferrite phase is soft and ductile, the lowest hardness value was obtained in the ferritic structure. The hardness increased and elongation decreased with the amount of pearlite phase in the microstructure since the pearlite phase contains lamellar Fe_3C . The upper bainitic structure has the highest hardness value of all matrix structures. As known, ausferrite is the main phase composed of ferrite and high-carbon retained austenite. At high austempering temperatures and long durations, the second stage reaction occurs in which high carbon retained austenite decomposes into carbide and ferrite. These carbides may cause an increase in hardness and a decrease in elongation. Parallely, the elongation value (3.96 %) is the lowest in the UB structure.

The tempered martensite has the highest 0.2 yield and ultimate tensile strength with low elongation values. Several reasons for this result may be; i) precipitation strengthening by cementite/alloy carbide precipitation, ii) decomposition of retained austenite into

ferrite and cementite, and iii) kinematic hardening arises from the plastic incompatibility between the matrix (ferrite) and secondary particles (cementite) [14].

Table 2. Mechanical properties of the matrix structures using unnotched samples.

Matrix	Hardness, (HB)	0.2 yield strength, (MPa)	Ultimate tensile strength, (MPa)	Elongation, (%)
F	175	345	502	10.94
P/F	226	470	635	8.37
P	255	490	682	7.1
TM	309	934	1147	5.32
LB	277	704	1025	13.12
UB	329	489	625	3.96

The tensile strengths of the circumferentially V-notched specimens and notch strength ratios (NSR) are given in Table 3. NSR values are calculated by dividing the notched tensile strength values by the unnotched tensile strength values. The F, P/F, and P structures showed NSR values greater than 1 for all notch radii. These structures have ductile ferrite phases alone or in combination and show high ductility (lower hardness and higher elongation). In ductile crystalline metals, the area between the notch root is more likely to deform plastically. This lowers the stress in that area and makes the notch radius less sharp or blunt. Because of this, the plastic deformation of ductile crystalline materials has been mostly limited in the area between the notch roots. Triaxiality stress in this area makes it easier for holes to form, which makes the sample with the notches fragile. On the other hand, they make the largest Mohr's stress circle small, which means that the average stress has to be higher than it was for the samples that weren't notched. This also has the effect of making the notch stronger [15, 16]. In the same way, Durmuş et al. [17] said that an NSR number greater than 1 means there is a lot of plasticity. Ultimately, the F, P/F, and P structures exhibiting elevated NSR values (exceeding 1) may be classified as notch-insensitive structures by having a strengthening mechanism in this study.

The NSR values of the 0.05 mm radius notched samples in F, P/F, and P structures exceed those of the 0.1 to 0.4 mm notched samples. This may result from increased strain hardening due to elevated triaxial stress and improved localized strength at the sharpest radius. Furthermore, localized residual stresses may develop during the fabrication or evaluation of the 0.05 mm notched samples, imparting enhanced strength near the notch tip and leading to an elevated NSR.

Tempered martensitic iron showed the lowest NSR values of all the matrixes. This can be attributed to the brittleness of the tempered structure in this study which has a low percent elongation value (5.32 %) showing sensitivity to the stress concentrations at the notched areas.

In all structures, the NSR increases with the notch radius. By increasing the notch radius, the stress concentration factor (K_t) decreases, reducing the local stresses at the notch tip and delaying the initiation of cracks due to the stress distributing over a larger area compared to the sharp notches with a small radius. These factors cause the structures to have lower-notch sensitivity and higher NSR values in high-notch radii samples.

Table 3. The notched tensile strengths and notch strength ratios of the matrix structures.

Matrix	Radius, (mm)	Notched-tensile strength, (MPa)	NSR	Matrix	Radius, (mm)	Notched-tensile strength, (MPa)	NSR
F	0.05	633.500	1.26195	TM	0.05	664.727	0.57953
	0.1	605.397	1.20597		0.1	648.529	0.56541
	0.16	603.836	1.20286		0.16	633.891	0.55265
	0.25	610.277	1.21569		0.25	736.352	0.64198
	0.4	613.789	1.22268		0.4	757.235	0.66018
	0.8	634.282	1.26351		0.8	996.701	0.86896
P/F	0.05	803.489	1.26533	LB	0.05	819.687	0.79969
	0.1	765.627	1.20571		0.1	812.466	0.79264
	0.16	749.428	1.18020		0.16	869.454	0.84824
	0.25	772.848	1.21708		0.25	871.991	0.85072
	0.4	771.287	1.21462		0.4	907.511	0.88537
	0.8	808.368	1.27302		0.8	1038.856	1.01352
P	0.05	788.461	1.15610	UB	0.05	573.976	0.91836
	0.1	742.793	1.08914		0.1	552.703	0.88432
	0.16	740.060	1.08513		0.16	504.107	0.80657
	0.25	758.406	1.11203		0.25	575.733	0.92117
	0.4	764.066	1.12033		0.4	629.012	1.00641
	0.8	816.369	1.19702		0.8	704.150	1.12664

In the multiple linear regression analysis the coefficient of determination (R^2), reflecting the correlation between the dependent variables (hardness, 0.2 yield strength, and notch radius) and NSR, was determined to be 0.896. This value indicates the validity of the multiple regression model, showing the linear relationship between dependent and independent variables. In multiple regression models, when a new independent variable is added, the R^2 value generally increases [18]. Therefore, the adjusted- R^2 value in multiple regression models is more important to be meaningful. The adjusted R^2 is 0.886 for the linear analysis, which means that 88.6 % of the change in the NSR is explained by predictor variables (hardness, 0.2 yield strength, and notch radius). The F value is 92.055, and the significance F is 8.02×10^{-16} .

The obtained linear regression model is given below in Eq. (1) where HB is Brinell hardness, $\sigma_{0.2}$ is 0.2 yield strength (MPa), and r is the radius of the centered V notch in mm. The notch radius factor, with a coefficient value of 0.21131, is the most significant term in the NSR model. Nonetheless, the hardness and 0.2 yield strength play a minor role in the NSR model.

$$NSR = 1.75715 - 0.0014 \times HB - 0.00077 \times \sigma_{0.2} + 0.21131 \times r \quad (1)$$

The P-level is the parameter that decreases as the confidence in the outcome increases. A greater P-level indicates a lower likelihood of dependency among the dataset variables. In most circumstances, a value of 0.05 is an appropriate threshold for statistical significance. Statistically significant outcomes possess a P value of 0.01, while statistically highly significant results have a P value of 0.005 or 0.001 [19]. The hardness,

0.2 yield strength, and notch radius have statistical significance (P-values are lower than 0.05) on the NSR model with P-values of 1.05×10^{-4} , 1.51×10^{-10} , and 1.89×10^{-4} , respectively. The high value of F (used to verify the significance of the regression) and the significance levels of P much lower than 0.001 show that the regression model is highly significant.

The predicted NSR values and residuals are given in Table 4 for the analysis. Residuals represent the discrepancies between the actual observed NSR values and the predicted NSR values generated by the model. They give a discussion of the error or deviation between the model's predictions and the actual results. Residuals are significant as they reflect the adequacy of the model's fit to the data. An effective model will provide residuals randomly distributed about zero, as illustrated in Table 4, indicating that the model consistently predicts the NSR accurately, free of any discernible trend of underestimation or overestimation. Large residuals signify that the model inadequately predicts NSR for specific data points, potentially indicating the necessity for further variables or nonlinear relationships.

Table 4. The predicted NSR values and residuals for the multiple linear regression analysis.

Matrix	Predicted NSR	Residuals	Matrix	Predicted NSR	Residuals
F	1.253220907	0.008729093	TM	0.606111546	-0.026581546
	1.263786743	-0.057816743		0.616677382	-0.051267382
	1.276465747	-0.073605747		0.629356385	-0.076706385
	1.295484252	-0.079794252		0.648374891	-0.006394891
	1.327181761	-0.104501761		0.680072399	-0.019892399
	1.411708451	-0.148198451		0.764599089	0.104360911
P/F	1.084220778	0.181109222	LB	0.83027332	-0.03058332
	1.094786614	0.110923386		0.840839156	-0.048199156
	1.107465617	0.072734383		0.853518159	-0.005278159
	1.126484123	0.090595877		0.872536665	-0.021816665
	1.158181631	0.056438369		0.904234173	-0.018864173
	1.242708321	0.030311679		0.988760863	0.024759137
P	1.027929787	0.128170213	UB	0.924842911	-0.006482911
	1.038495623	0.050644377		0.935408748	-0.051088748
	1.051174627	0.033955373		0.948087751	-0.141517751
	1.070193132	0.041836868		0.967106256	-0.045936256
	1.10189064	0.01843936		0.998803765	0.007606235
	1.18641733	0.01060267		1.083330455	0.043309545

Fig. 5 illustrates the tested and predicted results of the independent variables (hardness, 0.2 yield strength, and notch radius) on the NSR. Fig. 5a shows that the NSR decreases slightly as the hardness increases, indicating that higher hardness might reduce the notched strength ratio. The inverse relationship between hardness and NSR is also evident from the negative sign of the hardness variable coefficient (-0.0014) in the mathematical model given by Eq. 1. High matrix hardness provides low ductility, which means the plastic deformation at the notch root is more effectively prevented. As a result, crack formation accelerates, leading to a decrease in the NSR.

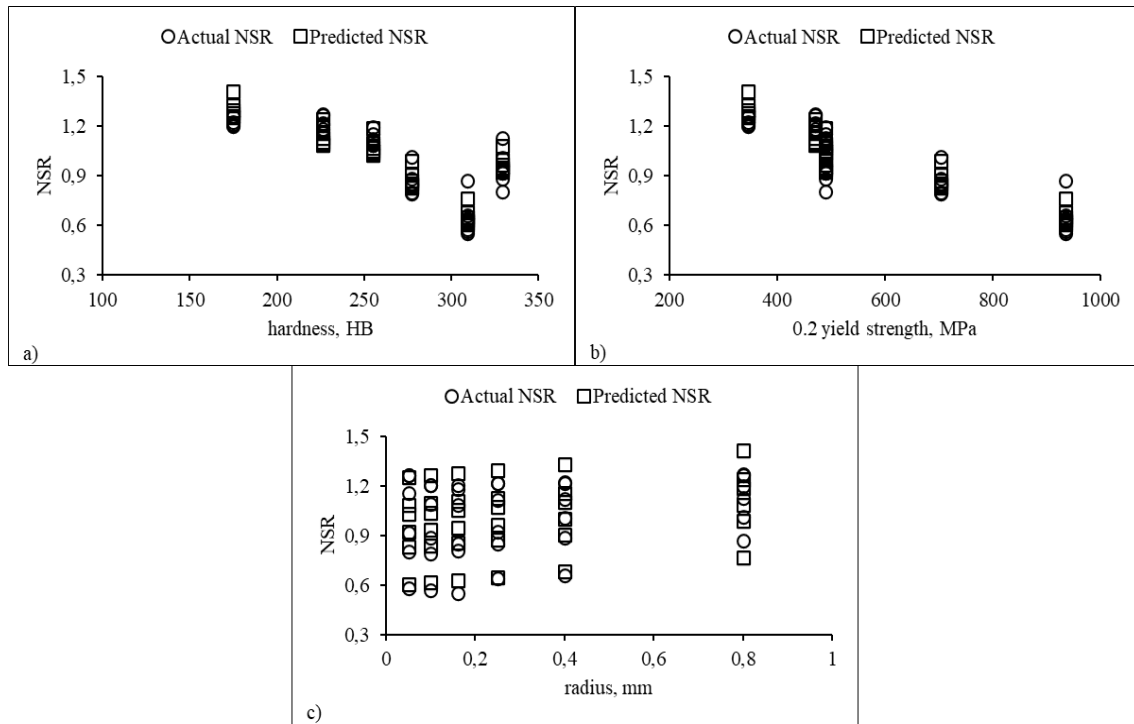


Figure 5. The tested and predicted results of the a) hardness, b) 0.2 yield strength, and c) radius on the NSR.

As the yield strength increases, the NSR seems to decrease, suggesting that materials with higher yield strength may have a lower NSR (Fig. 5b). It can be inferred from the minus sign of the yield strength coefficient (-0.00077) in Eq. 1. This means that the triaxial stress at the notch root will not exceed the high yield strength. This will inhibit the redistribution of local stresses by plastic deformation at the notch, cause premature failure, and diminish notched tensile strength, decreasing the NSR.

The NSR appears to be relatively increasing with the radius, with slight variations in the measured and predicted values (Fig 5c). As the notch radius increases, the stress concentration factor (K_t) decreases according to Eq. 2 where; a is the notch depth (mm), and r is the notch radius (mm) [20]. This is not the only but the simplest stress concentration factor formula showing the effect of notch radius on K_t . Many other formulas exist for specific geometries of notched parts. Generally, K_t and NSR are inversely correlated with each other. That is increasing K_t decreases NSR and vice versa. Low K_t means reduced peak stress at the notch root and more uniform distributed stress, making the notched and unnotched strengths closer, which results in a higher NSR.

$$K_t = 2 \sqrt{\frac{a}{r}} \quad (2)$$

The comparison of actual and predicted NSR indicates that our predictive model for NSR is largely consistent with the actual data but with minor discrepancies.

4. Conclusions

The influence of V-notched root radius and matrix structure on the NSR value of an alloyed ductile iron was examined experimentally. A predictive model was established using a multiple linear regression approach, including hardness, 0.2 yield strength, and notch radius as independent variables. The results can be drawn as follows:

- The F, P/F, and P structures demonstrated NSR values exceeding 1 for all notch radii, indicating that these matrix structures are notch insensitive.
- The notch radius improved NSR values for all matrix structures, except for a 0.05 mm radius. The NSR of the 0.05 mm radius notched condition was higher than that of the 0.1 mm for all matrix structures.
- The adjusted R^2 is 0.886, which indicates that the independent variables (hardness, 0.2 yield strength, and notch radius) can explain 88.6 percent of the change in the NSR. The P-values of independent variables are all lower than 0.001 showing that the regression model is highly significant.
- The predicted model yielded acceptable NSR predictions with minimal residuals. The model indicates that hardness and 0.2 yield strength exert an inverse influence, however, the notch radius positively affects the NSR.

References

- [1] T. Ikeda, N. Nodab, Y. Sano, Conditions for Notch Strength to be Higher Than Static Tensile Strength in High-Strength Ductile Cast Iron, **Engineering Fracture Mechanics**, 206, 75–88, (2019).
- [2] L. Collini, A. Pirondi, Microstructural, Multilevel Simulation of Notch Effect in Ferritic Ductile Cast Iron Under Low Cycle Fatigue, **International Journal of Fatigue**, 162, (2022).
- [3] H. T. Quraishi, M. A. Siddiqui, D. M. Naqvi, M. Zeeshan, M. Waseem, Z. Noreen, Machine Learning Prediction of Mechanical Properties in Reinforcement Bars: A Data-Driven Approach, **International Journal of Innovations in Science & Technology**, 6, 2, 413–425, (2024).
- [4] H. Yurtkuran, M. E. Korkmaz, M. Günay, Modelling and Optimization of the Surface Roughness in High-Speed Hard Turning with Coated and Uncoated CBN Insert, **Gazi University Journal of Science GU J Sci**, 29, 4, 987–995, (2016).
- [5] D. M. Jones, J. Watton, K. J. Brown, Comparison of Hot Rolled Steel Mechanical Property Prediction Models Using Linear Multiple Regression, Non-Linear Multiple Regression, and Non-Linear Artificial Neural Networks, **Ironmaking and Steelmaking**, 32, 5, 435–442, (2005).
- [6] K. A. Kasvayee, E. Ghassemali, I. L. Svensson, J. Olofsson, A.E.W. Jarfors, Characterization and Modeling of the Mechanical Behavior of High Silicon Ductile Iron, **Materials Science & Engineering A**, 708, 159–170, (2017).
- [7] L.P. Dix, R. Ruxanda, J. Torrance, M. Fukumoto, D.M. Stefanescu, Static Mechanical Properties of Ferritic and Pearlitic Lightweight Ductile Iron Castings, **AFS Transactions**, 03, 109, 1149–1164, (2003).
- [8] S. Biswas, C. Monroe, T. Prucha, Use of Published Experimental Results to Validate Approaches to Gray And Ductile Iron Mechanical Properties Prediction, **International Journal of Metalcasting**, 11, 4, 656–674, (2017).

- [9] D. Franzen, B. Pustal, A. Bührig-Polaczek, Influence of Graphite-Phase Parameters on The Mechanical Properties of High-Silicon Ductile Iron, **International Journal of Metalcasting** 17, 1, 4–21, (2023).
- [10] J. Laine, J. Vaara, K. Jalava, K. Soivio, J. Orkas, T. Frondelius, The Mechanical Properties of Ductile Iron at Intermediate Temperatures: The Effect of Silicon Content and Pearlite Fraction, **International Journal of Metalcasting** 15, 2, 538–547, (2021).
- [11] N. Ram, V. Gautam, Prediction of Effect of Alloying Elements on Properties of Ferritic Grade Si-Mo Ductile Cast Iron Using Regression Analysis, **Materials Today: Proceedings**, 62, 3855–3859, (2022).
- [12] G. Matache, A. Paraschiv, M. R. Condruz, Tensile Notch Sensitivity of Additively Manufactured IN 625 Superalloy, **Materials**, 13, 4859, (2020).
- [13] ISO 6506-1, Metallic materials-Brinell hardness test, Part 1: Test method, Switzerland, (2014).
- [14] L. Wang, Mechanical Properties of Tempered Martensite, PhD Thesis, Department of Materials Science and Engineering, Monash University Victoria, Australia, (2020).
- [15] R. Qu, P. Zhang, Z. Zhang, Notch Effect of Materials: Strengthening or Weakening?, **Journal of Materials Science and Technology**, 30, 6, 599–608, (2014).
- [16] C. Pandey, M.M. Mahapatra, P. Kumar, N. Saini, Effect of Strain Rate and Notch Geometry on Tensile Properties and Fracture Mechanism of Creep Strength Enhanced Ferritic P91 Steel, **Journal of Nuclear Materials**, 498, 176–186, (2018).
- [17] A. Durmus, H. Aydin, M. Tutar, A. Bayram, K. Yigit, Effect of the Microstructure on the Notched Tensile Strength of As-cast and Austempered Ductile Cast Irons, Proceedings of the Institution of Mechanical Engineers, Part C: **Journal of Mechanical Engineering Science**, (2012).
- [18] C. Hagquist, M. Stenbeck, Goodness of Fit in Regression Analysis – R^2 and G^2 Reconsidered, **Quality & Quantity** 32, 229–245, (1998).
- [19] A. A. Kanaeva, E. N. Reshetkinab, A. T. Kanaev, Use of the Multiple Regression Analysis for Quantitative Estimation of the Mechanical Properties of Strengthened Rebars, *Steel in Translation*, 49, 8, 568–573, (2019).
- [20] A. Bayram, A. Uguz, A. Durmus, Rapid Determination of the Fracture Toughness of Metallic Materials Using Circumferentially Notched Bars, **Journal of Materials Engineering and Performance**, 11, 5, 571–576, (2002).